HHS Public Access

Author manuscript

Clin Cancer Res. Author manuscript; available in PMC 2021 September 01.

Published in final edited form as:

Clin Cancer Res. 2021 March 01; 27(5): 1391–1398. doi:10.1158/1078-0432.CCR-20-2891.

Circulating Tumor Cell Subtypes and T-cell Population as Prognostic Biomarkers to Combination Immunotherapy in Metastatic Genitourinary Cancer Patients

Heather Chalfin[1], **Tiziano Pramparo**[2], **Amir Mortazavi**[3], **Scot A. Niglio**[1], **Joseph Schonhoft**[2], **Adam Jendrisak**[2], **Yen-Lin Chu**[2], **Robin Richardson**[2], **Rachel Krupa**[2], **Amanda Anderson**[2], **Yipeng Wang**[2], **Ryan Dittamore**[2], **Sumanta K. Pal**[4], **Primo N. Lara**[5], **Mark N. Stein**[6], **David Quinn**[7], **Seth M. Steinberg**[1], **Lisa M. Cordes**[1], **Lisa Ley**[1], **Marissa Mallek**[1], **Olena Sierra Ortiz**[1], **Rene Costello**[1], **Jacqueline Cadena**[1], **Carlos Diaz**[1], **James L. Gulley**[1], **William L. Dahut**[1], **Howard Streicher**[1], **John J. Wright**[1], **Jane B. Trepel**[1], **Donald P. Bottaro**[1], **Andrea B. Apolo**[1]

[1]National Cancer Institute, Bethesda, MD

[2]Epic Sciences, Inc., San Diego, CA

[3]Arthur G. James Cancer Hospital, Ohio State University Wexner Medical Center, Columbus, OH

[4]City of Hope, Duarte, CA

[5]University of California, Davis, Sacramento, CA

[6]Columbia University, New York, NY

[7]University of Southern California, Los Angeles, CA.

Abstract

Purpose: Circulating tumor cells (CTCs) are under investigation as a minimally invasive liquid biopsy that may improve risk stratification and treatment selection. CTCs uniquely allow for digital pathology of individual malignant cell morphology and marker expression. We compared CTC features and T-cell counts with survival endpoints in a cohort of metastatic genitourinary (mGU) cancer patients treated with combination immunotherapy.

Experimental Design: Markers evaluated included pan-CK/CD45/PD-L1/DAPI for CTCs and CD4/CD8/Ki-67/DAPI for T cells. ANOVA was used to compare CTC burden and T-cell populations across time points. Differences in survival and disease progression were evaluated using the maximum log-rank test.

Results: From 12/2016–01/2019, 183 samples from 81 patients were tested. CTCs were found in 75% of patients at baseline. CTC burden was associated with shorter OS at baseline (p=0.022) but not on therapy. Five morphologic subtypes were detected, and the presence of 2 specific subtypes with unique cellular features at baseline and on therapy were associated with worse OS (0.9–2.3

Corresponding Author: Andrea B. Apolo, National Cancer Institute, National Institutes of Health, 10 Center Dr., Rm. 13N240, Bethesda, MD 20892. Phone: 301-480-0536 Fax: 301-480-8867 andrea.apolo@nih.gov.

Disclosure of Potential Conflicts of Interest: None

mos vs. 28.2 mos,p<0.0001–0.013). Increasing CTC heterogeneity on therapy had a trend towards worse OS (p=0.045). PDL1+ CTCs on therapy were associated with worse OS (p<0.01,cycle 2). Low baseline and on-therapy CD4/CD8 counts were also associated with poor OS and response category.

Conclusions: Shorter survival may be associated with high CTC counts at baseline, presence of specific CTC morphologic subtypes, PD-L1+ CTCs, and low %CD4/8 T cells in mGU cancer patients. A future study is warranted to validate the prognostic utility of CTC heterogeneity and detection of specific CTC morphologies.

Keywords

Circulating Tumor Cells; Immunotherapy; Genitourinary Cancer; Bladder Cancer; Liquid Biopsy

Introduction

Circulating tumor cells (CTCs) are one of many liquid biopsies currently under investigation to improve risk stratification and optimize treatment selection for cancer patients in a minimally invasive fashion (1). To date, the majority of CTC research has relied on quantitative technology that simply counts the number of epithelial marker-positive cells detected from a peripheral blood sample (1, 2). However, a new generation of CTC technology is emerging that uses a combination of immunofluorescence microscopy and computer vision algorithms to assess CTC morphology and biomarker expression, allowing for direct evaluation of micrometastatic disease at the cellular level. This technology analyzes cell morphology of individual CTCs, similar to how a pathologist examines the cellular features of a solid tumor (3). The ability to describe a heterogeneous population of CTC subtypes seems especially valuable in the setting of primary tumor heterogeneity, whereas other liquid biopsies, such as circulating tumor DNA (ctDNA), can only report an averaged signal.

Ultimately, this work led to the novel biomarker “CTC heterogeneity,” which refers to the degree of uniformity of CTC subtypes expressed by an individual patient. Initial application of CTC subtyping and heterogeneity assessment in metastatic castration-resistant prostate cancer (mCRPC) revealed that patients with CTCs of more uniform size and shape had a better prognosis than those with greater heterogeneity of subtypes (4). Further, patients who displayed multiple CTC subtypes were more likely to respond to taxane chemotherapy vs. targeted therapy, suggesting a connection between the mutational burden that allows for resistance and the observation of more varied CTC morphologies. In a follow-up study, mCRPC patients with high CTC heterogeneity responded better to immunotherapy with ipilimumab and nivolumab (5). These early findings suggest that CTC heterogeneity could potentially function as a predictive biomarker for response to immunotherapy with checkpoint inhibition. One mechanistic hypothesis for this relationship is that the presence of many different cell morphologies might possibly act as a surrogate marker for tumor mutational burden (TMB). TMB has been widely studied as a putative biomarker for immunotherapy response, with measurements taken from tumor specimens as well as from ctDNA via liquid biopsy (6). Indeed, degree of CTC morphologic heterogeneity may be an

ideal candidate for a minimally invasive marker of predicted response to immunotherapy, with the additional advantage over ctDNA that PD-L1 expression can be assessed (7).

Expression of PD-L1 allows cancer cells to inhibit the antitumor response by inducing apoptosis of cytotoxic T cells and increasing regulatory T cells (8). Given these possible tumor-induced changes, in addition to traditional CTC detection we also applied the Epic Sciences rare cell detection platform to quantify and characterize peripheral blood T-cell populations in a cohort of metastatic genitourinary (mGU) cancer patients treated with the combination of cabozantinib and nivolumab with or without ipilimumab (Trial ID NCT02496208). Notably, cabozantinib may have immunomodulatory properties that counteract tumor-induced immunosuppression, providing a rationale for combining this agent with checkpoint inhibitors (9). In this study, we compared T-cell counts and CTC morphologic features at baseline and on therapy at cycle 2 and cycle 3 with progression-free survival (PFS), overall survival (OS), and response to combination therapy.

Matereials and Methods

Study design

This was a retrospective analysis of two cohorts of patients treated at 6 centers (National Institutes of Health; City of Hope; University of California; Ohio State University; Rutgers University; University of Southern California). The clinical outcomes of the phase 1 dose-escalation cohort have recently been reported (10). All patients provided signed informed consent to participate on a protocol approved by each institution's Institutional Review Board/Privacy Board prior to blood sampling, and studies were conducted in accordance with the Declaration of Helsinki, Belmont Report, and U.S. Common Rule. Blood draws were obtained at baseline (cycle 1 day 1 [−15 days allowed]; C1D1), cycle 2 day 1 (C2D1), and cycle 3 day 1 (C3D1).

Patients and treatment

From 07/20/2016–08/27/2019, 81 adult patients with mGU tumors were treated (Trial ID NCT02496208) with cabozantinib and nivolumab (n = 60) or cabozantinib, nivolumab, and ipilimumab (n = 21). CTCs were only collected during expansion cohorts with a set dose and schedule. Patients were required to have histologically confirmed metastatic urothelial carcinoma, clear cell renal cell carcinoma, adenocarcinoma of the bladder, squamous cell carcinoma of the penis, squamous cell carcinoma of the bladder, small cell carcinoma of the bladder, renal medullary carcinoma, sarcomatoid bladder and renal cell carcinoma, plasmacytoid carcinoma of the bladder, or other rare bladder/kidney cancer histology (Table 1). Metastatic disease was defined as new or progressive lesions on cross-sectional imaging with at least one site measurable by RECIST or bone disease by sodium fluoride PET-CT. Patients must have progressed on standard therapy or have no existing standard therapy for their disease, including cisplatin-ineligible urothelial cancer patients.

Sample collection and processing

Blood draws from each study participant were collected in cell-free preservative blood tubes (Streck; Omaha, NE) and shipped at room temperature to Epic Sciences (San Diego, CA) on

the same day of collection. Blood samples taken up to 96 hours previously were processed as previously described (3, 11, 12). Briefly, red blood cells were lysed using an ammonium chloride solution, and approximately 3×10^6 nucleated cells per slide were plated on up to 12 glass microscope slides (25.3 mm × 75.3 mm) and stored at −80°C until analysis. Samples were deemed invalid and were not processed if they arrived outside the 96-hour window, were damaged or drawn in an incorrect tube type, were of insufficient volume (< 4 mL), were clotted or hemolyzed, or were shipped at the wrong temperature (e.g., frozen). A total of 183 samples were processed, including 67 at baseline and 116 on therapy (60 C2D1 and 56 C3D1).

CTC and T-cell detection

Samples were analyzed using the Epic CTC platform, as previously described (12, 13). The CTC panel included pan-CK/CD45/DAPI/PD-L1 for CTCs and PD-L1-expressing CTC detection (14). Traditional CTCs were defined as cells (CK+, CD45−) with intact nuclei (DAPI), and were generally larger and morphologically distinct from surrounding white blood cells (3, 12). Positivity for the CTC panel was defined as a fluorescent signal above the defined analytical threshold established with cultured cell line control cells spiked into healthy donor blood, as previously described (3, 14). Negativity for CD45 was defined as having intensity below visual detection under the boundary condition that 99% of all cells are detectable globally (12). For PD-L1, the E1L3N clone was used. Cutoffs for positivity were established based on an analytical threshold of fluorescence using cell lines. Of the 67 baseline, 60 C2D1, and 56 C3D1 samples tested with the CTC panel, 63, 55, and 49, respectively, were also analyzed with a T-cell activation panel (all available material was tested). The T-cell activation panel included CD4/CD8/Ki-67/DAPI for analysis of subpopulations of immune cells. Positivity cutoffs for CD4 and CD8 were determined based on the local minimum between positive and negative peaks of cell counts by mean fluorescence intensity (MFI). The specificity of the activation panel was determined by multiple methods, including MFI assessment on positive and negative cells (immunomagnetically purified CD4+ or CD8+ cells), and co-localization with unique T-cell markers, such as CD3. The percentage values were calculated based on the number of CD4+ and CD8+ cells over the total number of DAPI+ cells. For both panels, each slide was imaged through automatic digital pathology pipelines to detect and quantify CTCs and immune cell populations.

CTC heterogeneity

We investigated CTC subtypes using a modification of the digital pathology pipeline previously implemented to quantify variability in CTC morphology of metastatic prostate cancer patients (4). Briefly, 2,527 CTC images from the mGU cohort were analyzed to measure nuclear and cytoplasmic morphologic features on a per-cell basis. Apoptotic CTCs were excluded from the analysis due to the limited ability of digital pathology features to recognize fragmented membrane and nuclei. Unsupervised K-means clustering of the CTCs along their digital pathology features was then used to sort CTCs into phenotypically similar subtypes from all samples. Here, “unsupervised” refers to the idea that the number of morphologies was not dictated at the beginning of the analysis. As CTC morphology is a novel idea, there is minimal published data available addressing whether the number of

subtypes and their defining features will remain consistent across different cancer types. For example, Scher *et al* identified 15 subtypes in metastatic prostate cancer (4). The number of clusters was selected by the "elbow" method to minimize "wide-sense stationary" (15) and the "silhouette" method to maximize the average cluster score (16). All CTCs in the cohort were assigned a phenotypic cell subtype (A–E) (Fig. 2A). Next, the patient-level frequency of the defined CTC phenotypic subtypes (categorized as A–E/mL) were determined per sample. CTC heterogeneity was measured using CTC subtype counts by calculating the Shannon Index (17).

Statistical analysis

Patient characteristics were evaluated by descriptive statistics. Analysis of variance was used to compare CTC burden and T-cell populations across time points and best response categories. Continuous variables with right-skewed distributions were transformed by log2(x + 1) to establish a normal distribution. Chi-squared tests were used to compare CTC subtype enrichment between urothelial cancer patients and other patients. Time-to-event outcomes, categorized by groups, were evaluated with the Kaplan-Meier method. Differences in survival and disease progression between categorized groups were evaluated using the maximum log-rank test. Due to the exploratory nature of this study, cutoff selection for survival analyses was optimized to obtain the largest differences; in other words, the results shown reflect the greatest effect possible and the p values associated with these analyses would need to be adjusted to account for the optimization, since the ones shown are the smallest possible p values which could be obtained without adjustments for the method used to determine the values. However, a cutoff of 4 CTC/mL (Fig. 1) is supported by previous investigations as a possible upper limit for the presence of CTCs in healthy donor blood (12). A cutoff of 1 CTC count per sample (Fig. 2) is supported by the scoring system used in the AR-V7 protein assay (4, 18-20). Cutoffs for CD4+ and C8+ white blood cells are currently being validated with independent study cohorts. Dynamic changes in Shannon Index were calculated by subtracting mean-normalized scores between 2 consecutive time points and by association with outcome using a cutoff of > or < 0. All statistical tests were 2-sided and were performed at the 5% significance level. Data consolidation was conducted using KNIME. Statistical analyses utilized the following R packages: survival, stats, vegan, and maxstat. Graphical representations were generated with the following R packages: ggplot2, gridExtra, scales, survminer, and ggthemes. Additionally, an identical sub-analysis was performed limiting solely to the urothelial histology patients.

Independent analysis using a different approach

To mitigate bias, an independent statistical analysis was performed at our institution (National Institutes of Health, author SMS; remainder of analysis was done by author TP, Epic Sciences) using a different approach to determine the way in which the patients would be separated into groups. In order to report findings which were not based on finding an optimal cut-off but rather one based on the distributions of the CTC values, it was decided beforehand that for each of 5 morphologic subtypes, patients would be separated into subgroups based on the number of detected CTCs of that subtype. Patients with 0 CTCs comprised one group; the other patients either comprised one group if < 15 patients were in the group or divided into 2 more groups of equal size if > 15 patients had values > 0. This

was done for each time point (baseline/C1D1, C2D1, and C3D1) using a Kaplan-Meier survival analysis for PFS and OS. Curves began at the time at which data were obtained; for example, CTC values available at cycle 2 were divided into groups and evaluated for association with OS or PFS beginning at cycle 2. These analyses were done using SAS version 9.4 (SAS Institute, Inc., Cary, NC).

Results

Clinical characteristics of study cohort

At baseline, 67 patients who had urothelial carcinoma (UC; n = 46) and other GU cancers (n = 21) were treated. Across all 81 patients, the median age was 63 years (range 20–82); 35 (69%) were male. N = 49 (75%) had visceral involvement, n = 24 (35%) had liver involvement, n = 17 (25%) had bone involvement, and n = 18 (27%) had lymph node involvement (Table 1). Fifty-one (76%) and 44 (66%) baseline patients, respectively, had C2D1 and C3D1 matched samples. Forty-nine cycle 2 patients (82%) had cycle 3 matched samples and 42 patients (52%) had matched samples at all 3 time points (Supplementary Fig. 1).

CTC enumeration

CTCs were found in the peripheral blood of 50 patients (75%) at baseline, 46 patients (77%) at C2D1, and 35 patients (62%) at C3D1. Median (range) CTC count/mL was 1.1 (0–216) at baseline, 0.9 (0–91) at C2D1, and 0.4 (0–19) at C3D1 (Fig. 1A). The decrease in total CTC count on therapy was not statistically significant (p = 0.061, Fig. 1B). Traditional CTC detection with a cutoff of > 4 CTCs/mL at baseline was associated with worse median OS (2.3 vs. 28.2 months (95% confidence interval [CI]: 0.95–inf vs. 16.28–inf); p = 0.022; Fig. 1C), but not on therapy. However, exploratory optimization with a higher CTC burden cutoff was indicative of worse survival at C2D1 (Supplementary Fig. 2). CTC burden was not significantly associated with PFS. Results of a sub-analysis limited to urothelial only histology were consistent with the overall analysis (Supplementary Fig. 3).

PD-L1+ CTCs

PD-L1+ CTCs were seen in 10% (n = 7) of patients at baseline, 17% (n = 10) at C2D1, and 4% (n = 2) at C3D1. Median (range) PD-L1+ CTC count/mL was 0 (0–0.9) at baseline, 0 (0–1.4) at C2D1, and 0 (0–0.9) at C3D1. The presence of PD-L1+ CTCs (> 0) was associated with worse median PFS at baseline (1.3 vs. 5.1 months; 95% CI: 0.76–inf vs. 3.1–22.1; p = 0.0039; Supplementary Fig. 4) and worse OS on therapy at C2D1 (4 vs. 28.2 months; 95% CI: 2.8–inf vs. 19.5–inf; p = 0.0091; Fig. 1D).

CTC morphologic subtypes

We identified 5 distinct morphologic subtypes (Fig. 2A). The characteristics of these 5 subtypes were as follows: A: medium CK intensity, smallest size, high circularity, low nuclear entropy and speckling, high nucleus-to-cytoplasm ratio; B: high CK intensity, low CK speckling, high circularity, low nucleus-to-cytoplasm ratio; C: very elongated cells, medium speckling, low nucleus-to-cytoplasm ratio; D: large cells, slightly elongated, high nuclear speckling and entropy; E: CTC clusters, slightly elongated, medium CK intensity

and speckling. At each time point, we saw no significant enrichment in CTC subtypes in urothelial cancer patients vs. other patients in this study, suggesting that these 5 subtypes may be pan-CTCs rather than urothelial CTCs specifically (Supplementary Table 1). All subtypes were found in the peripheral blood of patients with similar range of prevalence at all time points (from ~ 10% to 60%; Supplementary Table 2). Subtypes A and E were the most and least represented of all CTCs, respectively (Supplementary Table 3). The presence of subtype B was associated with shorter median OS at baseline (0.8 vs. 28.2 months; 95% CI: 0.62–inf vs. 16.3–inf; $p < 0.0001$) and at C2D1 (2 vs. 28.2 months; 95% CI: 1.6–inf vs. 19.5–inf; $p < 0.00088$; Fig. 2B), as well as worse PFS at baseline (0.95 vs. 4.6 months; 95% CI: 0.53–inf vs. 2.76–22.1; $p = 0.032$; Supplementary Fig. 5). Detection of subtype D at baseline was associated with shorter median OS (2.3 vs. 28.2 months; 95% CI: 0.95–inf vs. 16.3–inf; $p = 0.02$; Fig. 2B). No subtype attained significance for therapeutic response category at any time point. Increasing CTC heterogeneity on therapy (baseline to C2D1), as quantified by the Shannon Index, showed a trend towards worse OS (5.1 months vs. not reached; 95% CI: 4.4–inf vs. 24.7–inf; $p = 0.045$; Supplementary Fig. 6). For the sub-analysis limited to urothelial only patients, consistent results were found where the presence of subtype B was associated with shorter median OS at baseline and at C2D1, and detection of subtype D at baseline was associated with shorter median OS (Supplementary Fig. 3B-C).

Internal statistical analysis

Results of the NIH statistical analysis were consistent with the Epic Sciences analysis. The results were based on different divisions in the data so they would not be expected to match but could support the same general conclusions. In these separate analyses, subtype B was associated with a trend towards worse median OS at C2D1 ($p = 0.066$; Supplementary Fig. 7A) as well as worse PFS at baseline ($p = 0.023$; Supplementary Fig. 7B) and C3D1 ($p = 0.012$; Supplementary Fig. 7C). Detection of subtype D at all time points was associated with shorter median OS (baseline $p = 0.020$; Supplementary Fig. 7D; C2D1 $p = 0.048$; Supplementary Fig. 7E; C3D1 $p = 0.037$; Supplementary Fig. 7F).

T-cell populations

A cutoff of CD4% < 7 at baseline and C2D1 was associated with shorter OS and PFS (baseline OS 2.3 months vs. not reached; 95% CI: 1.45–inf vs. 24.7–inf; $p < 0.0001$; PFS 1.4 vs. 15.3 months; 95% CI: 1.2–3.6 vs. 5.3–inf; $p = 0.00028$; Fig. 3A; C2D1 OS 3.2 vs. 28.2 months 95% CI:2.3–inf vs. 24.7–inf; $p = 0.0013$; PFS 1.8 vs. 15.3 months; 95% CI: 1.4–inf vs. 4.5–inf; $p = 0.0026$; Fig. 3C). A cutoff of CD8% < 3 was associated with shorter survival at baseline (OS 5.9 vs. 28.2 months; 95% CI: 1.8–inf vs. 24.7–inf; $p = 0.019$; PFS 2.3 vs. 15.3 months; 95% CI: 1.4–inf vs. 4.6–inf; $p = 0.029$; Fig. 3B), but not at C2D1 nor C3D1 (Fig. 3D). CD4% < 7 at baseline and at C2D1 was associated with worse therapeutic response category (Anova, $p = 0.013$ and $p = 0.0044$; Figs. 3E and 3H), whereas CD8% < 3 had a trend towards worse therapeutic response (Anova, $p = 0.39$ and $p = 0.54$; Figs. 3F and 3G). For the sub-analysis limited to urothelial only patients, consistent results were found where a cutoff of CD4% < 7 at baseline and C2D1 was associated with shorter OS and PFS and a cutoff of CD8% < 3 was associated with shorter survival at baseline, but not at C2D1 (Supplementary Fig. 3D-E). Similarly, for the sub-analysis CD4% < 7 at baseline was still associated with worse therapeutic response category (Supplementary Fig. 3F).

Discussion

In this study we examined the prognostic value of CTC enumeration, identification of subtypes, and T-cell counts with outcomes from a prospective clinical trial of mUC and mGU patients treated with combination immunotherapy. CTCs were present in 75% of patients at baseline, and higher CTC burden (> 4) was associated with shorter OS. The percentage of patients with detectable CTCs is in line with previous studies of mUC across multiple detection platforms (7, 21, 22).

We describe 5 distinct morphologic subtypes of CTCs in this study. Subtypes B and D were associated with worse OS not specific to UC. There was no distinct urothelial signature found in the pattern of morphologic subtype expression compared to the other malignancies in our cohort, supporting the pan-cancer theory that certain cellular features are negatively prognostic across cancer types (23). Interestingly, subtype E which contains CTC clusters was rarely detected. Notably, the workflow of the CTC detection platform employed herein is by design minimally disruptive to CTC clusters. There is no enrichment step, nor size-based microfluidic or affinity capture and all nucleated cells are directly deposited on a glass slide and fixed for staining. As such, the data suggests that CTC clusters are rare in genitourinary malignancies. CTC morphologic subtype and the heterogeneity of expression of those subtypes may further enhance the performance of this biomarker, with special relevance for patients undergoing immunotherapy as there may be an association with CTC heterogeneity and TMB.

CTC heterogeneity, as measured by the Shannon Index, has been associated with survival and therapeutic response to immunotherapy, chemotherapy, and androgen-receptor signaling inhibitor targeted therapy in mCRPC patients (4, 5). Here, we found a trend toward worse OS for patients with increasing CTC heterogeneity while on therapy. A future study is warranted to determine whether CTC heterogeneity will have utility in other GU malignancies, or if the focus should rest on the detection of specific morphologies, which were significant biomarkers for survival in this study.

Immunotherapy with checkpoint inhibition has led to great interest in predictive markers for success, with candidates such as PD-L1 expression and immune-infiltrating tumor cells. Here, we studied PD-L1 expression on CTCs and applied rare cell detection technology to circulating T-cell populations. We saw that low CD4 and CD8 cell counts were negative prognosticators, presumably representing a suppressed immune response (8). Low counts at baseline and on therapy were associated with worse OS and, in some cases, with poor therapeutic response category. We also found that the detection of PD-L1+ CTCs was associated with worse OS. Of note, several PD-L1 tumor assays employ different antibody clones as well as different definitions and cutoffs for positivity (24).

This study was exploratory and hypothesis-generating, and these findings must be confirmed in an independent homogeneous cohort. The results as shown reflect the optimal effects and need to be interpreted in that context. The NIH analysis was not optimized but reflected similar findings. The present cohort included a heterogeneous group of GU tumors, including a small number of rare histologies. As such, it was not possible to perform a sub-

analysis for each histologic type due to small numbers. Each cancer type has a different PFS and OS, thus it is a limitation to evaluate these endpoints for a combined cohort. Future studies would ideally include a greater number of patients, especially to further evaluate PD-L1+ CTCs, as these are known to be rarely expressed and were only exhibited in a small subset of the patients in this cohort (7). T-cell detection was based on CD4/8; however, it is known that there is some minimal expression of these markers on other peripheral blood cells (25).

In conclusion, our analysis found CTCs in mGU patients at baseline and on therapy with combination immunotherapy. Patients with CTCs > 4, specific CTC morphologic subtypes, PD-L1+, and low CD4 and CD8 T-cell counts had shorter survival. Future study is warranted to validate the prognostic utility of CTC heterogeneity.

Supplementary Material

Refer to Web version on PubMed Central for supplementary material.

Acknowledgments

This project has been funded with federal funds from the National Cancer Institute, National Institutes of Health.

References

1. van der Toom EE, Verdone JE, Gorin MA, Pienta KJ. Technical challenges in the isolation and analysis of circulating tumor cells. Oncotarget 2016;7:62754–66. [PubMed: 27517159]
2. de Bono JS, Scher HI, Montgomery RB, Parker C, Miller MC, Tissing H, et al. Circulating tumor cells predict survival benefit from treatment in metastatic castration-resistant prostate cancer. Clin Cancer Res 2008;14:6302–9. [PubMed: 18829513]
3. Werner SL, Graf RP, Landers M, Valenta DT, Schroeder M, Greene SB, et al. Analytical Validation and Capabilities of the Epic CTC Platform: Enrichment-Free Circulating Tumour Cell Detection and Characterization. J Circ Biomark 2015;4:3. [PubMed: 28936239]
4. Scher HI, Graf RP, Schreiber NA, McLaughlin B, Jendrisak A, Wang Y, et al. Phenotypic Heterogeneity of Circulating Tumor Cells Informs Clinical Decisions between AR Signaling Inhibitors and Taxanes in Metastatic Prostate Cancer. Cancer Res 2017;77:5687–98. [PubMed: 28819021]
5. Boudadi K, Suzman DL, Anagnostou V, Fu W, Luber B, Wang H, et al. Ipilimumab plus nivolumab and DNA-repair defects in AR-V7-expressing metastatic prostate cancer. Oncotarget 2018;9:28561–71. [PubMed: 29983880]
6. Snyder A, Morrissey MP, Hellmann MD. Use of Circulating Tumor DNA for Cancer Immunotherapy. Clin Cancer Res 2019;25:6909–15. [PubMed: 31285372]
7. Anantharaman A, Friedlander T, Lu D, Krupa R, Premasekharan G, Hough J, et al. Programmed death-ligand 1 (PD-L1) characterization of circulating tumor cells (CTCs) in muscle invasive and metastatic bladder cancer patients. BMC Cancer 2016;16:744. [PubMed: 27658492]
8. Ostroumov D, Fekete-Drimusz N, Saborowski M, Kuhnel F, Woller N. CD4 and CD8 T lymphocyte interplay in controlling tumor growth. Cell Mol Life Sci 2018;75:689–713. [PubMed: 29032503]
9. Apolo AB, Nadal R, Tomita Y et al. Cabozantinib and peripheral immunity in advanced urothelial carcinoma: Final results from an open-label, phase 2 trial. Lancet Oncol, 2020 Vol 21, 8, p 1099–1109. [PubMed: 32645282]
10. Apolo AB, Nadal R, Girardi DM, et al. Phase I Study of Cabozantinib and Nivolumab Alone or With Ipilimumab for Advanced or Metastatic Urothelial Carcinoma and Other Genitourinary Tumors. J Clin Oncol. 2020 9 11:JCO2001652. doi:10.1200/JCO.20.01652. Online ahead of print. PMID: 32915679

11. Punnoose EA, Ferraldeschi R, Szafer-Glusman E, Tucker EK, Mohan S, Flohr P, et al. PTEN loss in circulating tumour cells correlates with PTEN loss in fresh tumour tissue from castration-resistant prostate cancer patients. Br J Cancer 2015;113:1225–33. [PubMed: 26379078]
12. Marrinucci D, Bethel K, Kolatkar A, Luttgen MS, Malchiodi M, Baehring F, et al. Fluid biopsy in patients with metastatic prostate, pancreatic and breast cancers. Phys Biol 2012;9:016003. [PubMed: 22306768]
13. Marrinucci D, Bethel K, Lazar D, Fisher J, Huynh E, Clark P, et al. Cytomorphology of circulating colorectal tumor cells:a small case series. J Oncol 2010;2010:861341. [PubMed: 20111743]
14. Boffa DJ, Graf RP, Salazar MC, Hoag J, Lu D, Krupa R, et al. Cellular Expression of PD-L1 in the Peripheral Blood of Lung Cancer Patients is Associated with Worse Survival. Cancer Epidemiol Biomarkers Prev 2017;26:1139–45. [PubMed: 28446544]
15. Kintigh K Intrasite spatial analysis: a commentary on major methods. In: Voorrips A, editor. Mathematics and Information Science in Archaeology: A Flexible Framework. 3rd ed. Bonn, Germany: Holos; 1990. pp. 165–200.
16. Rousseeuw P Silhouettes: A graphical aid to the interpretation and validation of cluster analysis. J Comput Appl Maths 1987;20:53–65.
17. Shannon C A mathematical theory of communication. Bell Syst Tech J 1948;27:379–423.
18. Scher HI, Lu D, Schreiber NA, Louw J, Graf RP, Vargas HA, et al. Association of AR-V7 on Circulating Tumor Cells as a Treatment-Specific Biomarker With Outcomes and Survival in Castration-Resistant Prostate Cancer. JAMA Oncol 2016;2:1441–9. [PubMed: 27262168]
19. Beltran H, Jendrisak A, Landers M, Mosquera JM, Kossai M, Louw J, et al. The Initial Detection and Partial Characterization of Circulating Tumor Cells in Neuroendocrine Prostate Cancer. Clin Cancer Res 2016;22:1510–9. [PubMed: 26671992]
20. Graf RP, Hullings M, Barnett ES, Carbone E, Dittamore R, Scher HI. Clinical Utility of the Nuclear-localized AR-V7 Biomarker in Circulating Tumor Cells in Improving Physician Treatment Choice in Castration-resistant Prostate Cancer. Eur Urol 2020;77:170–7. [PubMed: 31648903]
21. Chalfin HJ, Glavaris SA, Gorin MA, Kates MR, Fong MH, Dong L, et al. Circulating Tumor Cell and Circulating Tumor DNA Assays Reveal Complementary Information for Patients with Metastatic Urothelial Cancer. Eur Urol Oncol 2019 9 25 [Online ahead of print].
22. Zhang Z, Fan W, Deng Q, Tang S, Wang P, Xu P, et al. The prognostic and diagnostic value of circulating tumor cells in bladder cancer and upper tract urothelial carcinoma: a meta-analysis of 30 published studies. Oncotarget 2017;8:59527–38. [PubMed: 28938656]
23. Huang HC, Chiang SJ, Wen SH, Lee PJ, Chen HW, Chen YF, et al. Three-dimensional nucleus-to-cytoplasm ratios provide better discrimination of normal and lung adenocarcinoma cells than in two dimensions. J Biomed Opt 2019;24:1–4.
24. Apolo AB. PDL1: The Illusion of an Ideal Biomarker. Eur Urol Focus 2016;1:269–71. [PubMed: 28723398]
25. Uhlen M, Fagerberg L, Hallstrom BM, Lindskog C, Oksvold P, Mardinoglu A, et al. Proteomics. Tissue-based map of the human proteome. Science 2015;347:1260419. [PubMed: 25613900]

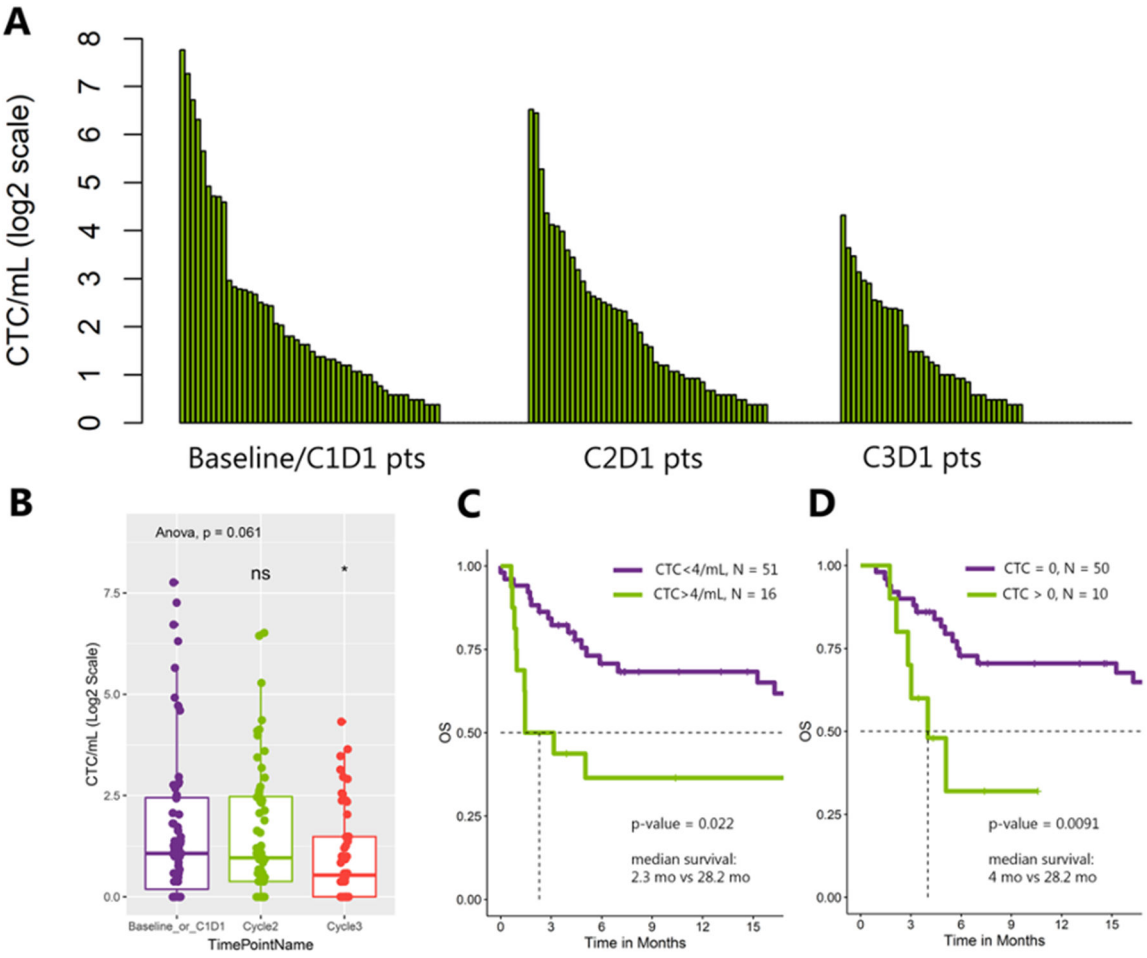

Figure 1. CTC burden and survival analysis

A) CTC count by patient across 3 time points (baseline, C2D1, C3D1). Patients are ordered by high to low CTC burden in each time point. **B)** Total CTC burden by time point. **C)** Kaplan-Meier curve at baseline with traditional CTC cutoff of 4/mL. **D)** Kaplan-Meier curve at C2D1 for PD-L1+ CTCs with a CTC cutoff of 0.

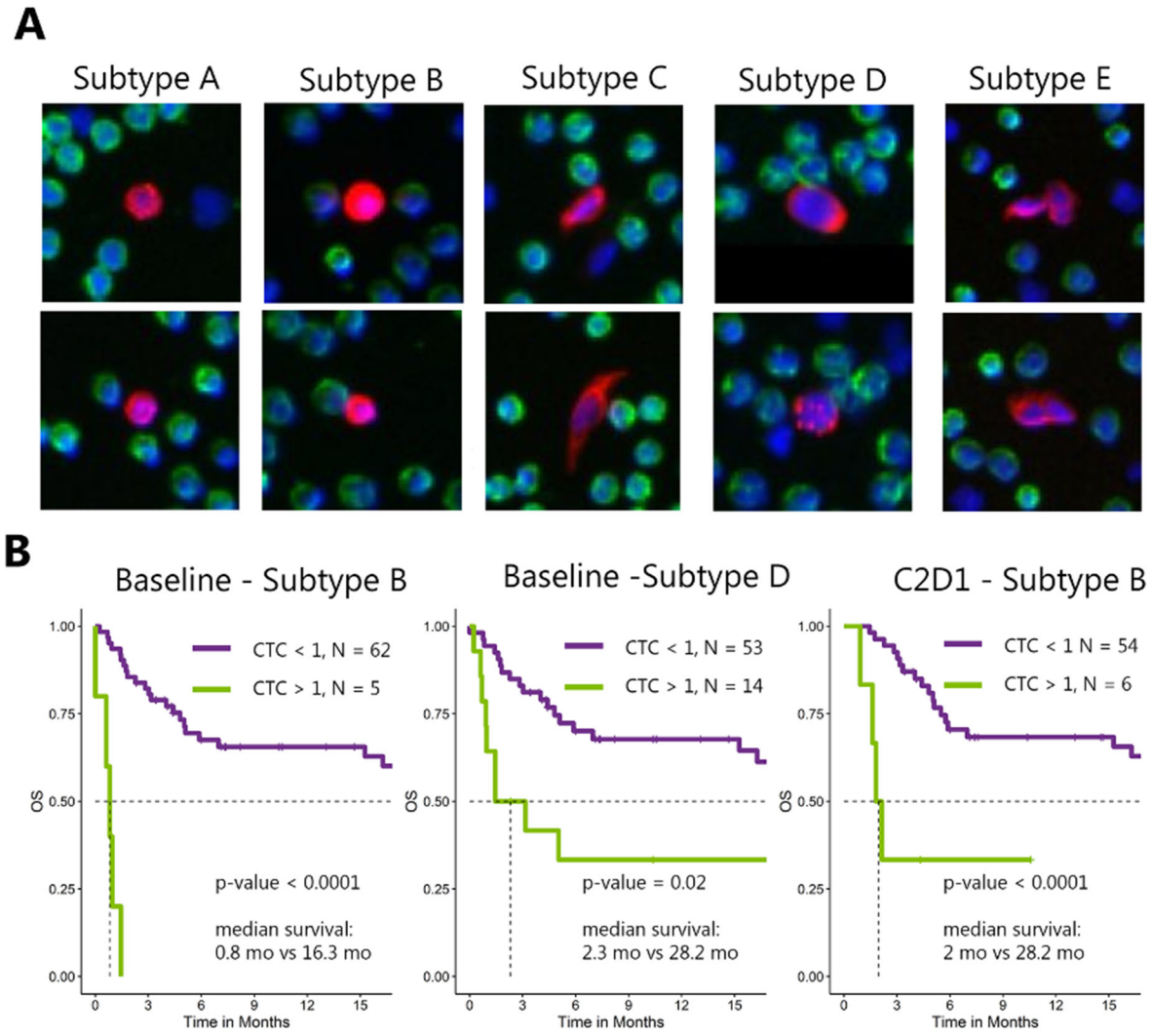

Figure 2. Morphology-based CTC subtypes and survival analysis

A) Unsupervised clustering using digital pathology features clustered CTCs into 5 subtypes (A–E) with distinct cell morphology (see Methods). **B)** Kaplan-Meier curves at baseline and C2D1 with CTC subtypes using a cutoff of 1 cell detected in one mL of blood.

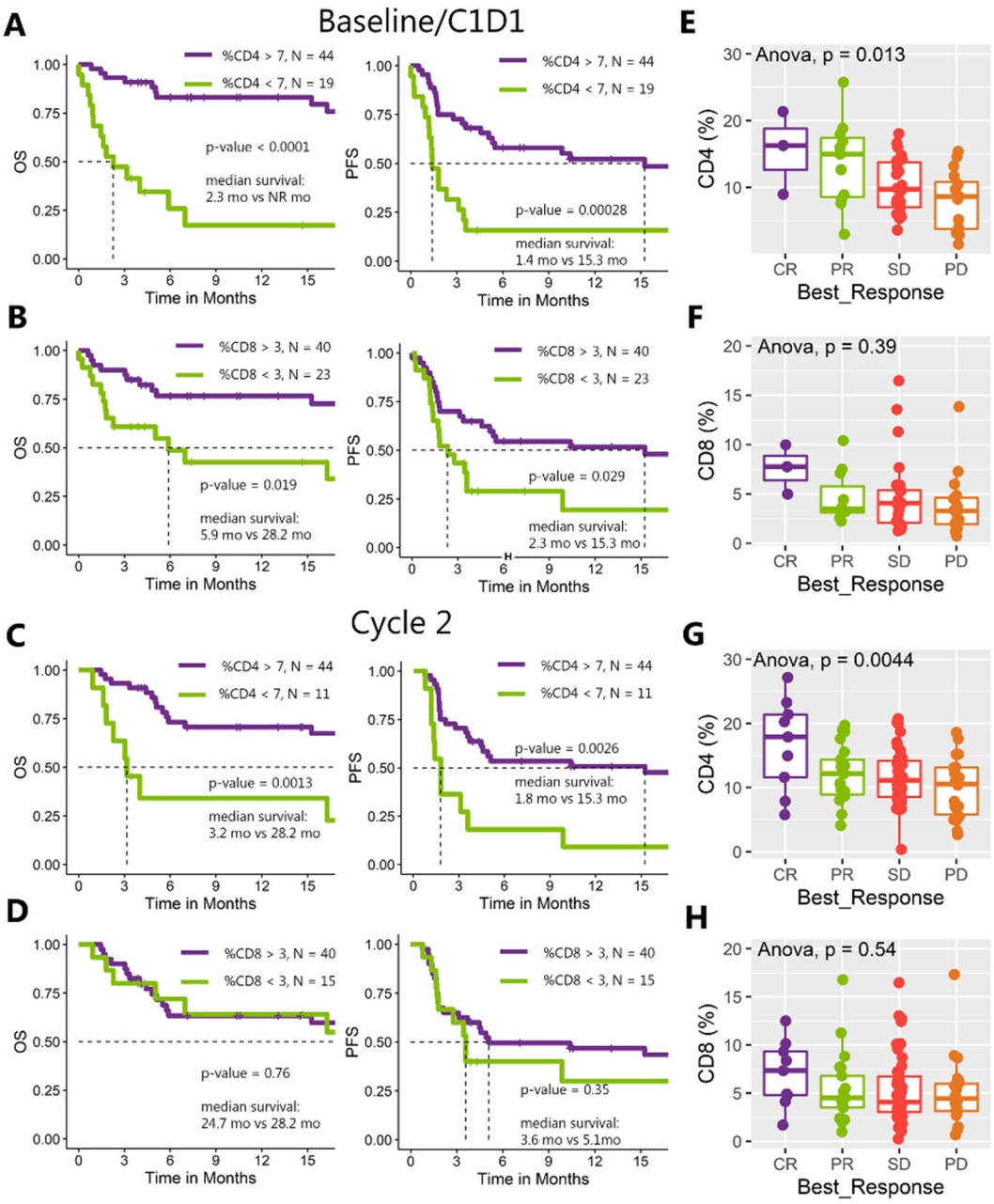

Figure 3. Survival analysis and therapeutic response by T-cell population

A, B) Kaplan-Meier curves for OS and PFS at baseline with white blood cells positive for CD4 and CD8 below cutoff of 7% and 3%, respectively. **C, D)** Kaplan-Meier curves for OS and PFS at C2D1 with white blood cells positive for CD4 and CD8 below cutoff of 7% and 3%, respectively. Cutoffs are exploratory and were optimized for this cohort (see Methods). **E–H)** Analysis of variance for CD4+ and CD8+ T-cell populations across the different categories of treatment response (E, F at baseline, G, H at cycle 2).

Table 1.

Patient characteristics. Sample counts and percentage by cancer and metastasis subtype.

Patient Characteristics	**n = 81**
Age in Years (range)	62 (20–82)
Male/Female (%)	69.1/30.9
Cancer Type – N (%)	
Urothelial	35 (43.2)
Urothelial - renal pelvis	16 (19.8)
Bladder Adenocarcinoma	9 (11.1)
Bladder Squamous Cell	6 (7.4)
Penile	3 (3.7)
Bladder Small Cell	2 (2.5)
Urothelial - Plasmacytoid Variant	1 (1.2)
Renal Medullary	2 (2.5)
Renal Clear Cell	4 (4.9)
Sarcomatoid Renal Cell	1 (1.2)
Chromophobe Renal Cell	1 (1.2)
Urachal Adenocarcinoma	1 (1.2)
Mets Type – N (%)	
Lymph Node	20 (24.69)
Visceral Mets	61 (75.31)
Liver Mets	27 (33.33)
Bone Mets	23 (28.40)